# Optical coherence tomography in clinical examination of non-pigmented skin malignancies

Jensen, LK; Thrane, L; Andersen, PE; Tycho, A; Pedersen, F; Andersson-Engels, Stefan; Bendsoe, N; Svanberg, Sune; Svanberg, Katarina

[Link to publication](#)

# Optical Coherence Tomography in Clinical Examination of Non-Pigmented Skin Malignancies

Laura K. Jensen[(1)(2)], Lars Thrane[(1)], Peter E. Andersen[*(1)], Andreas Tycho[(1)], Finn Pedersen[(1)], Stefan Andersson-Engels[(3)(6)], Niels Bendsøe[(4)(6)], Sune Svanberg [(3)(6)], Katarina Svanberg[(5)(6)]

[(1)]Optics and Fluid Dynamics Department, Risø National Laboratory, P.O. Box 49, DK-4000 Roskilde, Denmark
[(2)]Center for Communications, Optics and Materials, Technical University of Denmark, DTU Building 345v, DK-2800 Kgs. Lyngby, Denmark
[(3)]Department of Physics, Atomic Physics Division, P.O. Box 118, SE - 221 00 Lund, Sweden
[(4)]Department of Dermatology, Lund University Hospital, SE-221 85 Lund, Sweden
[(5)]Department of Oncology, Lund University Hospital, SE-221 85 Lund, Sweden
[(6)]Lund Medical Laser Centre

## ABSTRACT

Optical coherence tomography (OCT) images of basal cell carcinomas (BCCs) have been acquired using a compact handheld probe with an integrated video camera allowing the OCT images to be correlated to a skin surface image. In general the healthy tissue of the skin has an obvious stratified structure, whereas the cancerous tissue shows a more homogenous structure. Thus it was demonstrated that it is possible to distinguish BCCs from healthy tissue by means of OCT. Furthermore different histological types of BCC were identified. Comparison of OCT images taken prior to and immediately after photodynamic therapy clearly shows the tissue response to the treatment, and indicates local oedema in the treated area.

Keywords: Optical coherence tomography, basal cell carcinoma, photodynamic therapy, human skin

## 1. INTRODUCTION

During recent years the incidence of skin malignancies has increased. For the non-pigmented lesions there are a number of treatment modalities. Since topical application of δ-aminolevulinic acid (ALA) was introduced, photodynamic therapy (PDT) has been considered one way of treating these tumours. However, there are some limitations when applying PDT with distant surface illumination and topical sensitisation both from the ALA diffusion point of view as well as from light penetration. Therefore, it is of importance to determine the tumour thickness in the planning of the treatment. For example, for nodular basal cell carcinomas (nBCCs) it is often needed to apply PDT more than once. Another possibility is to perform cryosurgery, curettage or some other tumour thickness reducing modality before PDT is performed.

Palpation and visual inspection are the clinical ways of determining the extension and thickness of non-pigmented skin lesions, provided there has not been performed a punch biopsy. In this study, a non-invasive way to visualise the tumour thickness by means of OCT[1, 2] has been investigated in connection with ALA-PDT. This study has been focused on BCCs as it is the most common type of non-pigmented skin cancer. Furthermore it has been shown in other clinical studies the at BCC is suitable as a biological model for developing other diagnostic techniques, such as flouresence,[3, 4] Raman spectroscopy[5, 6] and laser Doppler.[7]

## 2. METHODS

OCT is based on low-coherence interferometry by using a broadband light source in a Michelson interferometer.[1, 2] The sample under investigation is placed in one arm of the interferometer and a reference mirror in the other arm. An interference signal arises only when the optical pathlength difference of the two arms is within the short coherence length of the source. A controlled optical delay scanning in the reference arm creates a single depth scan, also called an A-scan, and adjacent A-scans form an OCT-image or a B-scan.

---

[*] Correspondence: E-mail: peter.andersen@risoe.dk; WWW: http://www.risoe.dk; Telephone: + 45 4677 4555; Fax: + 45 4677 4565
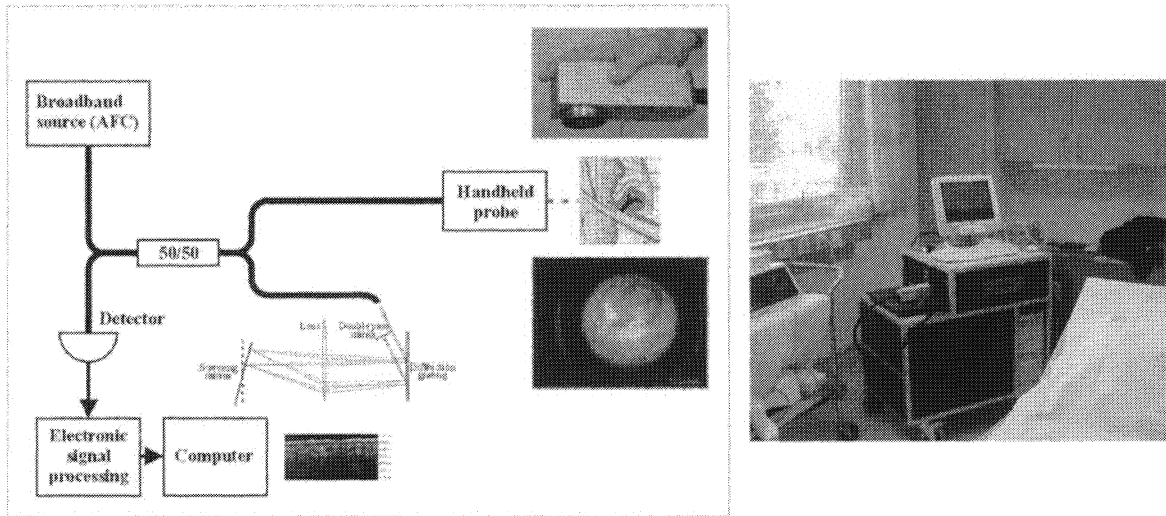
Fig. 1. Sketch of the mobile OCT system and compact handheld probe with integrated video camera (left). The video image of the skin shows the 4 mm scan line. The size of the probe is seen to be equal to the human hand. The mobile OCT system is shown in the clinical setting (Department of Oncology, Lund University Hospital) (right).

The images for this project have been acquired using a mobile OCT system in the clinic. A compact handheld probe with an integrated video (CMOS) camera was used to locate the lesion and acquire the OCT scan. Each cross-sectional OCT image is correlated with a video image of the skin surface, which helps to document the OCT images for later identification and evaluation. Nine patients with 12 BCC lesions were scanned immediately before and after the PDT procedure at the Department of Oncology, Lund University Hospital. The images were compared already during the clinical session to assess the tissue reaction to the treatment. Later detailed evaluation was performed.

The mobile OCT system used in the clinic has been implemented in fibre optics, mainly for compactness and robustness. The depth scan is accomplished by using a Fourier domain rapid scanning optical delay line (RSOD) in the reference arm.[8] For dermatological applications a compact handheld probe with an integrated video camera has been implemented in the sample arm. The size of the probe is approximately 15×7×5 cm (Figure 1). An OCT image of 400 A-scans across 4mm is acquired and saved along with a video image of the skin surface in approximately 5-6 seconds. The system employs a broadband light source (AFC BSS 1310 B), with centre wavelength at 1310 nm and a bandwidth of 60.4 nm, which in this set-up gives an axial resolution in the skin of 10 μm, lateral resolution of 26 μm, and a penetration depth of 1-1.5 mm (Figure 1). The dynamic range of the system is >100 dB. The handheld probe and an example of a skin surface image from the integrated video camera are shown in Figure 1 together with a block diagram of the mobile OCT system, as well as the clinical setting (Department of Oncology, Lund University Hospital).

In order to make the OCT images easier to interpret, image smoothing and structure enhancement have been performed by processing the images with the rotating kernel transformation (RKT) algorithm,[9, 10, 11] with kernels of size 11x11 pixels and a thickness of three pixels. For the images in this study the RKT images themselves do not improve the image quality, but enhances the stratified structure of healthy skin. The original OCT images have therefore been overlaid with the RKT images, in order to view both overall structures as well as details.

## 3. RESULTS

The purpose of the study was to investigate the usefulness of OCT for optical diagnosing of skin cancer. In order to differentiate the diseased areas from healthy tissue it is necessary to identify the characteristics of normal healthy skin. The normal tissue is then compared to different types of BCCs.

Downloaded from SPIE Digital Library on 04 Jul 2011 to 130.235.188.41. Terms of Use: http://spiedl.org/terms
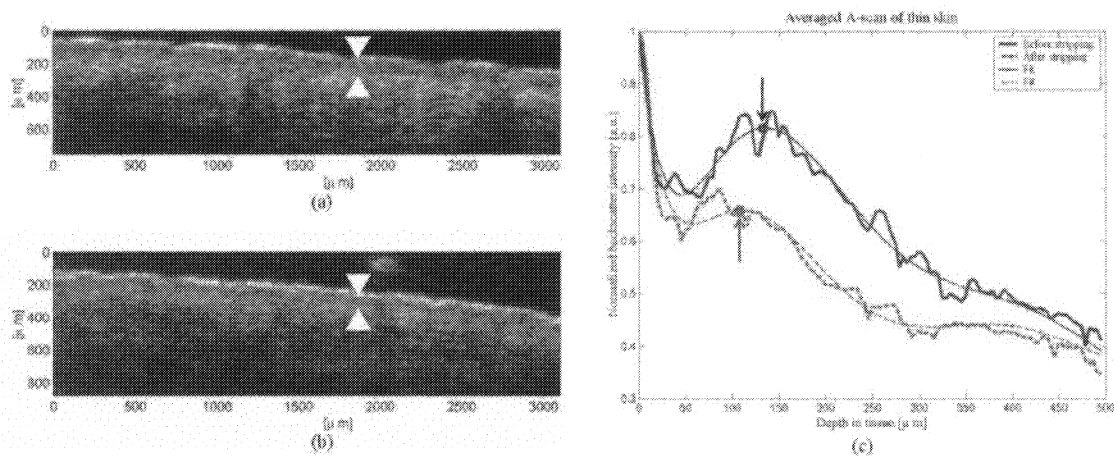
Fig. 2. OCT images of the volar forearm (left). The triangles mark the thickness of the epidermis before (a) and after (b) stripping of the skin. In (c) the A-scans of (a) and (b) have been aligned, averaged and normalized, and it is seen that the second peak (arrows), corresponding to the outer dermis, is closer to the surface of the skin.

## 3.1. Identification of layers in healthy skin

In healthy skin, the tissue is build up of several distinct layers; the epidermis forming an outer shield from the rest of the world, the dermis providing nutrients for the upper layers of the skin and giving the skin its flexibility, and beneath the subcutis, protecting the muscles from mechanical and thermal damage.[12, 13] The epidermis has several sublayers, which are formed during a process called keratinisation. As the skin cells mature they move towards the surface, they gradually become flattened and eventually they die. Forming the boundary to the dermis is the basal cell layer, stratum basale, where new cubical cells are produced. In the layer above stratum basale, stratum spinosum, the cells become dense, and in stratum granulosum the flattened cells have accumulated granules of keratin, making this layer more compact. The outermost layer, stratum corneum, is entirely made up of dead cells. The dermis has two layers, dermis papillare and dermis reticulare, both containing collagen and elastin fibres. Dermis papillare holds small blood vessels bringing nutrients to the epidermis, and the dermis reticulare contains such structures as hair follicles, sweat and sebaceous glands and larger blood vessels. Due to the fact that collagen is highly scattering the light of the OCT system is rarely returned from the subcutis, which is therefore seldom seen in OCT images. Depending on the location of the skin, the thickness varies a great deal, conditioned by the stress the particular site is exposed to; hence the eyelids have epidermal thickness of only 50 µm and dermal thickness of 300 µm, whereas the palms and soles have epidermal thickness up to 1.5 mm and the trunk have dermal thickness of up to 3 mm. Most of the human body is covered with so called thin skin, whereas the skin of the palms and soles is called thick skin.

OCT images of thin skin of the volar forearm are illustrated in Figure 2(a) and (b). Only three lateral structures can be clearly distinguished; topmost a white band, below a darker band, and in the lower part of the image a brighter area that fades with the depth, indicating that the separate layers of the epidermis and the dermis cannot be told apart from each other. To be certain that the topmost white band did not correspond to any histological layer, the volar forearm was imaged before (Figure 2(a)) and after (Figure 2(b)) stripping the skin, using application and quick removal of bandage tape a 100 times. It is seen that the white band has not been thinned out. This band corresponds to the entrance signal of the skin, since the surface reflection is relatively high compared to backscattering from lower parts of the tissue. By aligning and averaging the A-scans in both images it can be seen (Figure 2(c)) that the second peak (arrows) in the signal has been shifted closer to the surface. This second peak matches the outer dermis. Due to the fact that the epidermis has been thinned, the distance between the surface and the second peak is smaller after the skin stripping. Thus the upper darker band corresponds to the epidermis, which has been marked with triangles (Figure 2(a) and 2(b)).
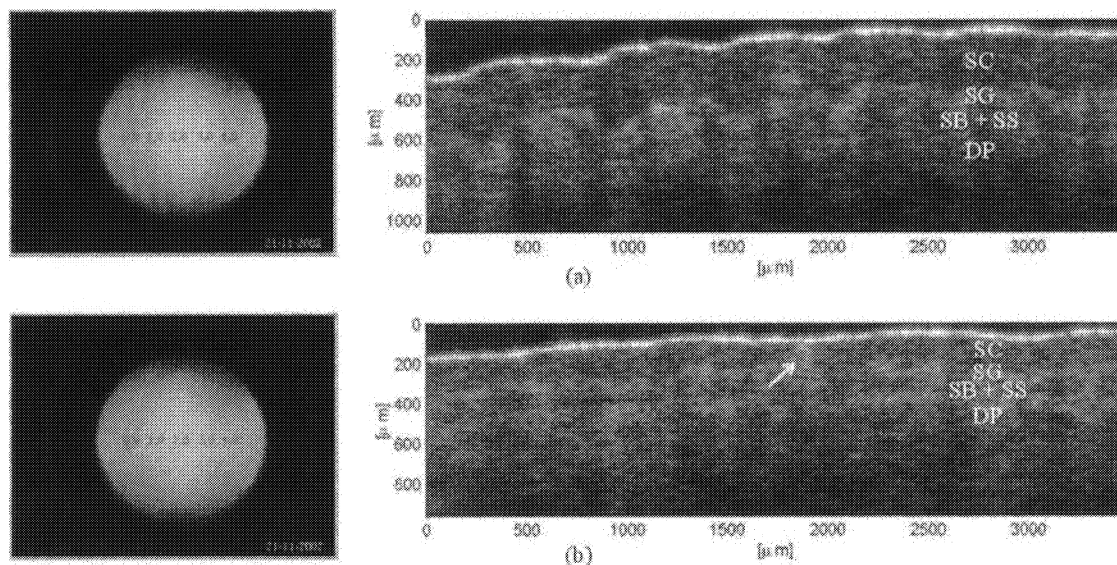
Fig. 3. Two OCT images and corresponding video images of thick skin in the palm. In both OCT images the different layers of the skin can be distinguished; Stratum Corneum (SC), Stratum Granulosum (SG), Stratum Basale and Stratum Spinosum (SB+SS) and the dermis (DP). In (a) the folds of the skin surface are clearly seen in the video image and in the OCT image the rete ridges can be recognized. In (b) the rete ridges are not so obvious. In the middle of the OCT image (arrow) a sweat gland duct is observed.

OCT images of thick skin in the palm are demonstrated in Figure 3. The thick skin has more visible layers than thin skin, and by comparing to earlier studies[14, 15, 16] the layers in Figure 3 can by identified. Stratum corneum (SC) is seen as a thick dark band just below the bright surface signal. Beneath this stratum granulosum (SG) with higher backscattering is visualised. Stratum basale (SB) and stratum spinosum (SS) lies underneath as a dark irregular band forming the boundary to the dermis papillare (DP). The dermis is seen as a brighter area that fades as the light is attenuated in the tissue. In Figure 3(a), the so-called rete ridges, the folds of the dermis reaching into the epidermis, are large enough to be clearly distinct, and even smaller structures, such as a sweat gland duct can be seen in Figure 3(b) marked with an arrow. The video image (a) shows the folds of the skin from the fingerprint analogous to the waves of the surface signal in the OCT image. In (b), the video image shows an even surface corresponding to the smooth surface signal seen the OCT image.

### 3.2. Scar tissue

Due to the recurrent nature of BCC, tumours sometimes occur in scars from the earlier treatment, especially if treated with cryosurgery or curettage, whereas PDT leaves less severe scars. As BCC can evolve in scar tissue, it is of importance to be able to distinguish normal scar tissue from recurrent BCC developing in scar tissue. Figure 4 illustrates a recurrent BCC on the forehead (a) and scar tissue of a BCC treated with cryosurgery (b) in the vicinity of the recurrent BCC. Both images show delimited areas of very fine grains, marked with dotted ellipses. These are supposedly cross-sections of collagen bundles. In healthy skin the collagen fibres in the dermis are distributed randomly, but in the healing process of a wound, the collagen fibres become more structured, and can form fibre bundles. The OCT images in Figure 4 apparently seem similar, but where the recurrent BCC has a homogenous structure apart from the marked areas, the scar tissue has a stratified structure, similar to that of normal skin.

Both deep and shallow scars have been scanned in this study, and all show more or less distinct areas with fine grains. How distinct these areas are also seems to depend on the freshness of the scar. Newly formed scar tissue (one month) shows hardly any such areas, whereas old scars (two years) show clearly delimited areas of fine grains. Lack of the same phenomenon in normal skin precludes that these areas are blood vessels, as they should be present in both normal skin and scar tissue. The upper layer is marked with triangles in Figure 4(b).
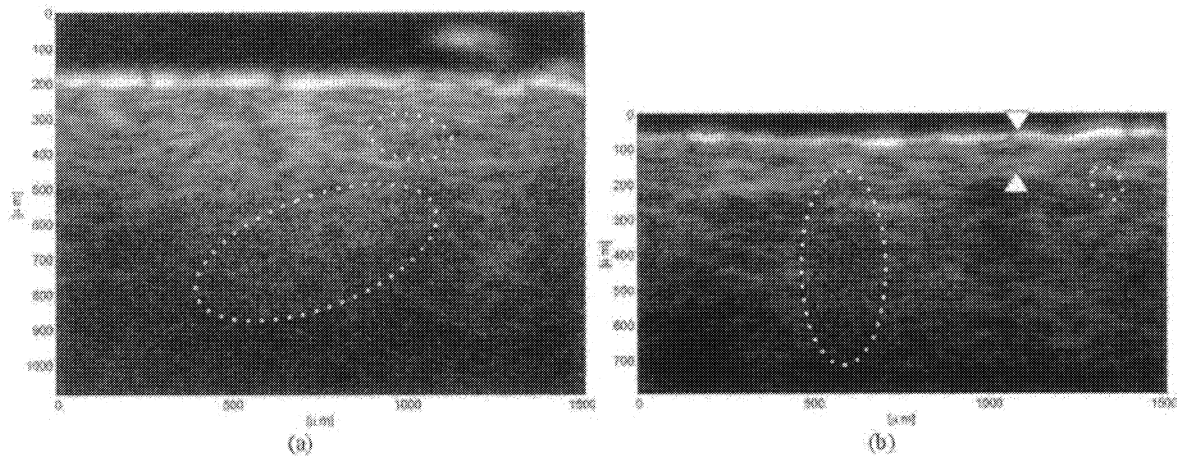
Fig. 4. OCT images of (a) a recurrent BCC on the forehead, and (b) scar tissue of an earlier treated BCC. Both images demonstrate areas with seemingly smaller grains (marked with dotted ellipses), but the scar tissue still shows a stratified structure (upper layer between triangles), whereas the BCC shows a homogenous backscattering.

## 3.3. Basal cell carcinoma

BCCs develop as masses of basaloid cells (cells similar to those in stratum basale), which reach into the dermis in more or less well-defined lobules or strands. The different clinical types of BCCs have in common the destruction of the layered structure of the skin as they progress,[13] which results in a more homogenous structure in the cancerous tissue. Figure 5 shows an OCT image of a superficial BCC on the leg (a), and an image of healthy skin in the vicinity of the BCC (b). In Figure 5(a) a hair causes a shadow through the image; neither the hair nor the shadow is a sign of disease. The indication of BCC is given by lack of the stratified structure in seen Figure 5(b), where the dermis (D) is clearly distinguishable from the epidermis (E) marked between the triangles.

It is occasionally possible to determine the lateral boundary of the BCC by locating the end of the stratified structure. In
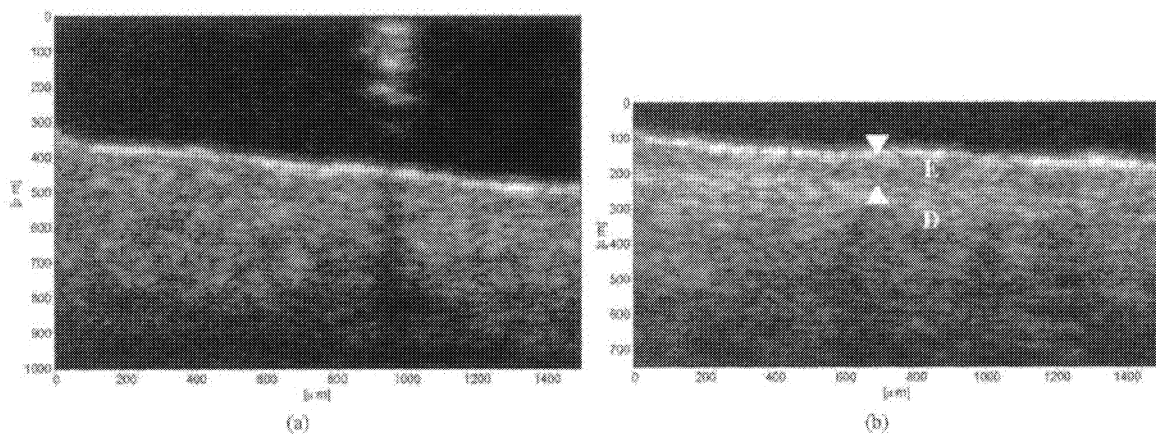


Fig. 5. OCT images of a superficial BCC on the leg (a), and healthy tissue in the vicinity of the lesion (b). In (a) a hair is causing a shadow through the image, which is not a sign of disease. By comparing the two images it is seen that the cancerous tissue homogenously backscatters the light, whereas in the healthy tissue the epidermis (E) and the dermis (D) are still distinct separate layers.
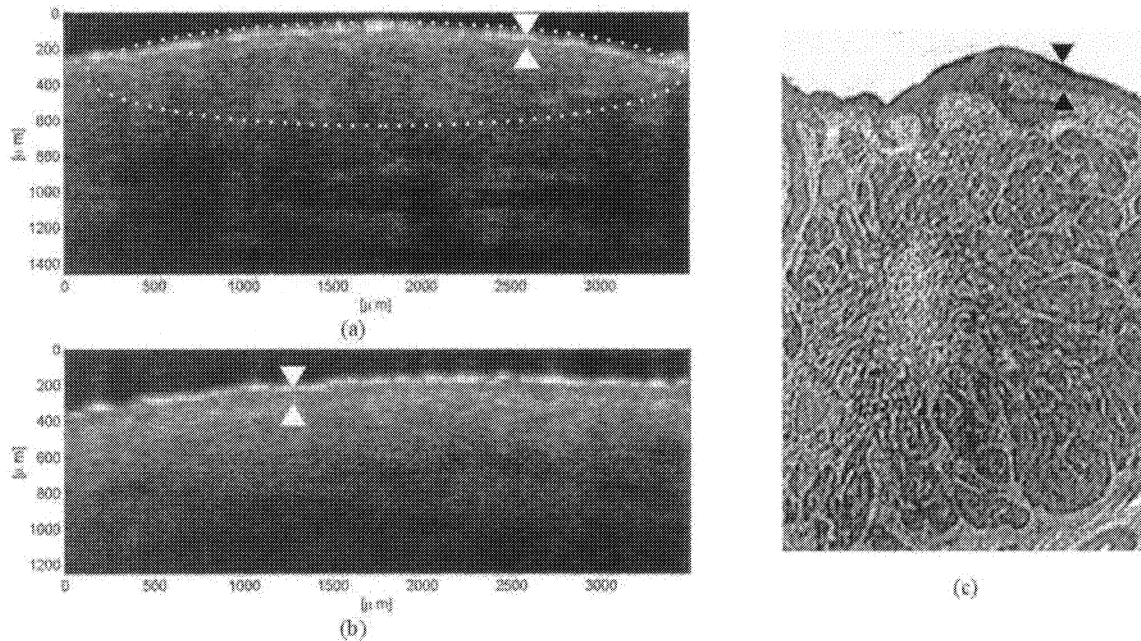
Fig. 6. OCT images showing a stratified BCC (a) marked with dotted ellipse, and healthy skin in the vicinity of the lesion (b). The triangles mark the thickness of the epidermis, and it is seen that though it is thinner in (a) than in (b) it is still intact. A histopathological section of a similar stratified lesion, where the intact epidermis is also marked is seen in (c).[17]

Figure 6(a) both the lateral and the axial boundaries can be identified, as a somewhat higher backscattering inside the dotted ellipse. Evidently the axial boundary can only be determined when the thickness of the lesion is less than the penetration depth of the light from the OCT system, which is restricted 0.5-1.5mm.

In the example in Figure 5, the epidermal layers are completely destroyed, but in certain cases the stratified structure of the skin is kept while the BCC spreads from stratum basale, as in Figure 6(a). Figure 6(a) shows a superficial BCC on the chest and 6(b) shows the normal skin in the vicinity of the BCC. It is seen that the epidermis is still intact in the cancerous area in contrast to the BCC shown in Figure 5(a). The thickness of the epidermis is marked with triangles in both images, and it is seen that the epidermis in the cancerous area is thinner than in the healthy tissue. In certain cases of BCCs where the stratified structure is kept while the cancer progresses, the epidermis is thinned out until it evolves into a wound. Figure 6(c)[17] illustrates a histopathological section of a similar stratified BCC to the one in 6(a), showing the intact epidermis between the triangles.

Occasionally BCC develops as isolated nests of basaloid cells in the dermis.[13] This is shown in Figure 7, where a recurrent BCC on the cheek has developed as clearly demarcated areas in the dermis. The nests are seen as dark spots marked with arrows in Figure 7(a), and can easily be distinguished from the connective tissue of the dermis, which is highly backscattering. It is also seen in Figure 7(a) that the epidermis is still intact. A histopathological section of a similar BCC lesion, with isolated well-defined large nests of basaloid cells, is given in Figure 7(b).

### 3.4. Photodynamic therapy
BCCs treated with topically application of ALA and laser light irradiation, where scanned before and immediately after the treatment. Figure 8 shows OCT images scanned before (a), and after (b) PDT with ALA. It is seen that the tissue clearly responds to the treatment by accumulation of fluids in the treated area caused by the chemical reactions in the cells, which makes the scatteres seem larger after PDT.
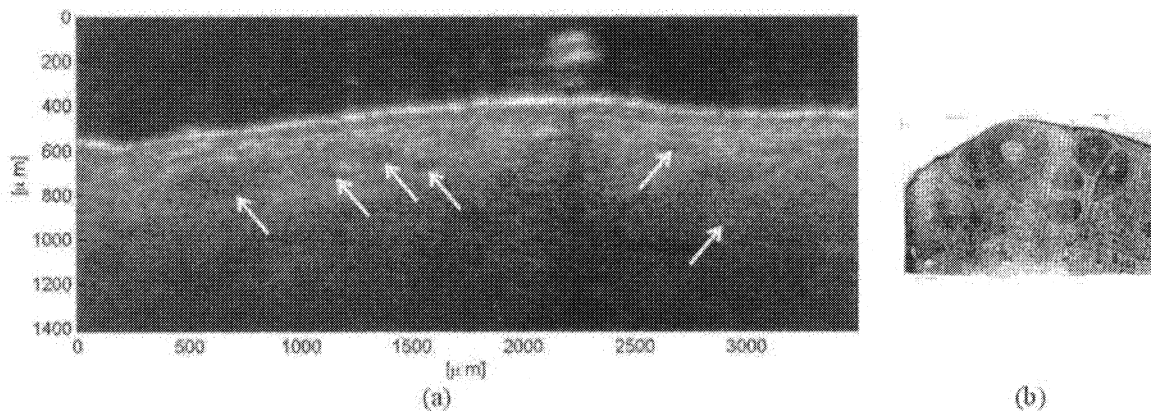
Fig. 7. The images show nests of tumour cells in dermis. In the OCT image (a) the areas are marked with arrows. The nests can easily be distinguished from the connective tissue of the dermis and the epidermis is still intact. In (b) is shown a histopathologic image of a similar lesion.[13]

Earlier studies using optical Doppler tomography (ODT)[19, 20] show that PDT with benzoporphyrin derivate (verteporfin®) and hematoporphyrin derivate (photofrin®) causes blood vessel diameter and blood flow to decrease shortly after ended irradiation. This might be due to the fact that sensitizers are also bound to the endothelium in the blood vessels. This is true if the sensitizer is administrated systematically. Results from these studies cannot be compared to the present study as the drug was distributed by topical application, which increases the blood flow during PDT and more indicates a cytotoxic effect.[8] An increased blood flow could not be distinguished from the OCT images.
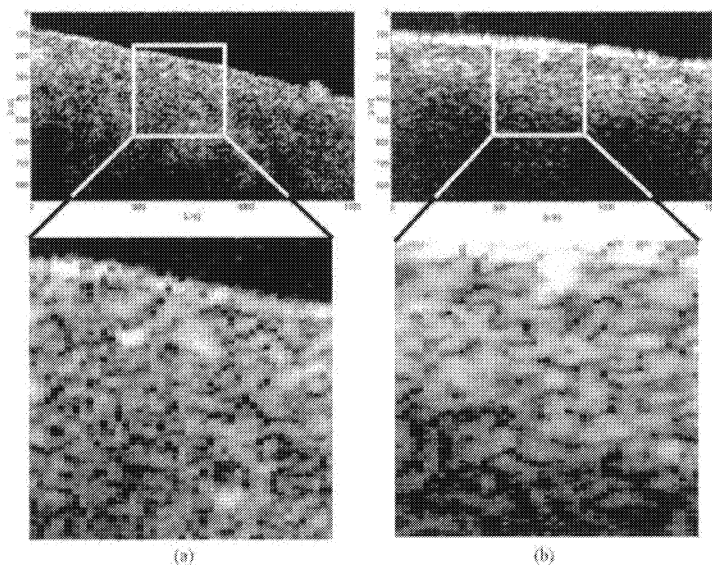


Fig. 8. The images demonstrate the photochemical reactions in the tissue after PDT. The tissue before the treatment (a), and immediately after (b) is shown. The grains are larger after the treatment corresponding to an oedema with "swollen" cells.

# 4. CONCLUSION

In conclusion, a number of BCC lesions have been imaged using a mobile OCT system and a compact handheld probe. Histological data have been successfully deduced from these images as a first step in correctly interpreting clinical dermatological OCT images. In healthy tissue an obvious stratified structure has been identified, which breaks down as BCC evolves. Depending on the type of BCC and the state of progression the cancerous areas can be seen as a homogenous area in the OCT images, occasionally under a thin but intact epidermis. In certain cases isolated nests of cancer cells can be identified in the dermis. It has been shown that it is possible to distinguish between recurrent BCC and scar following cryosurgery, which at a first glance seems similar, containing areas of fine grains. Still the scar tissue shows a stratified structure similar to normal skin, whereas the recurrent BCC shows as a homogenous region. In certain cases, it has been possible to deduce the lateral boundaries of the lesions from the OCT images, but due to the lack of penetration depth, the thickness of the tumours can only be determined by means of OCT for very superficial BCCs.

# ACKNOWLEDGEMENT

# REFERENCES

1. D. Huang, E.A. Swanson, C.P. Lin, J.S. Schuman, W.G. Stinson, W. Chang, M.R. Hee, T. Flotte, K. Gregory, C.A. Pulaifito, J.G. Fujimoto, "Optical Coherence Tomography", Science, **254**, 1178 (1991).
2. B.E. Bouma, G.T. Tearney (editors), "Handbook of Optical Coherence Tomography", Marcel Dekker Inc., 2002.
3. C. af Klinteberg, A.M.K. Enejder, I. Wang, S. Andersson-Engels, S. Svanberg and K. Svanberg, "Kinetic fluorescence studies of 5-aminolaevulinic acid-induced protoporphyrin IX accumulation in basal cell carcinomas", J. Photochem. Photobiol. B **49**, 120 (1999).
4. R. Cubeddu, A. Pifferi, P. Taroni, G. Valentini, G. Canti, C. Lindquist, S. Andersson-Engels, S. Svanberg, I. Wang and K. Svanberg, "Multispectral and lifetime imaging for the detection of skin tumors, in Biomedical Optical Spectroscopy and Diagnostics / Therapeutic Laser Applications", eds. E.M. Sevick-Muraca, J.A. Izatt and M.N. Ediger, Proc. OSA Trends in Optics and Photonics vol. **22**, 106 (1998).
5. S. Pålsson, N. Bendsøe, K. Svanberg, S. Andersson-Engels, S. Svanberg, "Near Infrared Raman spectroscopy for in vivo characterisation of skin lesions", Submitted to Photochem Photobiol (2003).
6. M. Gniadecka, H.C. Wulf, O.F. Nielsen, D.H. Christiansen, J. Hercogova, "Distinctive molecular abnormalities in benign and malignant skin lesions: studies by Raman spectroscopy", Photochem. Photobiol, **66**, 418 (1997).
7. I. Wang, S. Andersson-Engels, G.E. Nilsson, K. Wårdell and K. Svanberg, "Superficial blood flow following photodynamic therapy of malignant skin tumours measured by laser Doppler perfusion imaging", Br. J. Dermatol. **136**, 184 (1997).
8. A.M. Rollins, M.D. Kulkarni, S. Yazdanfar, R. Ung-arunyawee, J.A. Izatt, "In vivo video rate optical coherence tomography", Optics Express, **3**, 219 (1998).
9. J. Rogowska, C.M. Bryant, M.E. Brezinski, "Cartilage thickness measurements from optical coherence tomography", J.Opt. Soc. Am., **20**, 357 (2003).
10. J. Rogowska, M.E. Brezinski, "Image processing techniques for noise removal, enhancement and segmentation of cartilage OCT images", Phys. Med. Biol., **47**, 641 (2002).
11. Y.-K. Lee, W.T. Rhodes, "Nonlinear image processing by a rotating kernel transformation", Optics letters, **15**, 1383 (1990).
12. G.F. Murphy, "Dermaphathology", W.B. Saunders Company, 1995.
13. C.B Jaworsky, D.E. Johnson, E. Elenitsas, "Lever's Histopathology of skin", chap. 30, Lippincott-Raven Publishers, 1997.
14. J. Welzel, "Optical coherence tomography in dermatology: a review", Skin Research and Technology, **7**, 1 (2001).
15. A. Pagnoni, A. Knüttel, P. Welker, M. Rist, T. Stoudemayer, L. Kolbe, I. Sadiq and A. M. Kligman, "Optical coherence tomography in dermatology," Skin Research and Technology, **5**, 83 (1999).
16. A. Knüttel, M. Boehlau-Godau, "Spatially confined and temporally resolved refractive index andscattering evaluation in human skin performed with opticalcoherence tomography", Journal of Biomedical Optics, **5**, 83 (2000).
17. T.V. Rajan, M.D. UCHC, http://radiology.uchc.edu/code/1736.HTM.
18. Z. Chen, T.E. Milner, X. Wang, S. Srinivas, J.S. Nelson, "Optical Doppler Tomography: Imaging *in vivo* Blood Flow Dynamics Following Pharmacological Intervention and Photodynamic Therapy", Photochemistry and Photobiology, **67**, 56 (1998).
19. A. Major, S. Kimel, S. Mee, T.E. Milner, D.J. Smithies, S.Srinivas, Z. Chen, J.S. Nelson, "Microvascular Photodynamic Effects Determined *In Vivo* Using Optical Doppler Tomography", IEEE Journal of Selected Topics in Quantum Electronics, **5**, 1168 (1999).